CHAPTER 16

REVIEW OF CLASSICAL CONTROL DESIGN

draft draft

16.1 Introduction

[...]

16.2 Attitude control of a spacecraft

The typical purpose of putting a satellite into orbit is to point an instrument at something. The instrument, called payload, can be a telescope if an astronomy mission is designed or a camera/radar for an Earth observation satellite or a transmitting/receiving antenna for a telecommunications satellite. This implies that the attitude of the spacecraft must be stabilised to some desired attitude which is compatible with the task to be performed. Achieving a desired attitude requires the capability of *controlling* the attitude.

Passive methods of attitude control can be used by exploiting the natural system dynamics to ensure a stable equilibrium at the desired attitude. They are very useful and effective when accuracy requirements are coarse. Instead, when pointing accuracy is high, typically passive stabilisation is not enough and the spacecraft is equipped with an active attitude control system. The best solution is to design a spacecraft having passive natural stability, which is augmented if necessary with an active control system. In this way, the control system does not need to work as hard to maintain the required attitude. As any active control system, a spacecraft attitude control consists of attitude sensors and actuators and a processor capable of implementing the control law which relates the measured attitude and the corrective torques[1].

A fully comprehensive analysis of the three-dimensional attitude control of a spacecraft is beyond the aims of the present notes. However, some basic relevant control tools can be presented and discussed on a simplified configuration, namely the single-axis rotation of a satellite. In particular, the following simplified model is considered (see Figure 16.1). The spacecraft is assumed to be composed of a central rigid body of moment of inertia J_0 and two identical appendages of length ℓ, which may represent solar panels or spacecraft booms. The system can undergo rotational manoeuvres about

[1]Note that spacecraft motion is composed both by a translation and a rotational component. The translation part is related to orbital mechanics. In this notes, we restrict our analysis to the rotational motion governing the spacecraft attitude. Therefore, for our purposes, only the attitude dynamics is of interest.

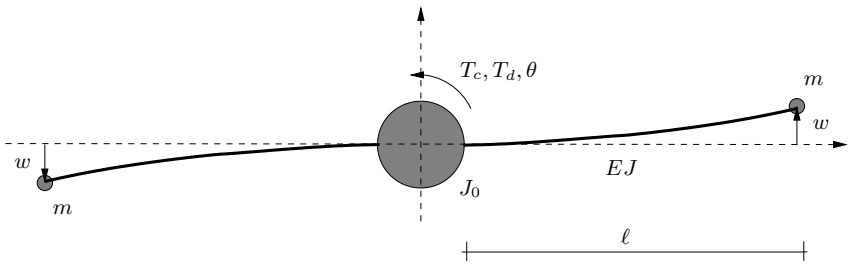

Figure 16.1 A simplified spacecraft rotating about a single axis.

the axis passing through the centre of mass of the central body. For the sake of simplicity, each appendage is modelled as a lumped-parameter system consisting of a massless beam of flexural rigidity EJ carrying a point mass m at the tip. The central body is equipped with a sensor measuring the rotation $\theta(t)$ and an actuator capable of providing a control torque T_c (for example, a pair of rocket thrusters). A disturbance torque T_d is also applied on the central body. Many external torques act on a spacecraft which disturb the attitude motion. They include magnetic torque, solar radiation pressure torque, aerodynamic torque and gravity-gradient torque. In our simplified analysis, all these effects are expressed by the disturbance torque T_d.

16.2.1 System modelling (rigid case)

The design of the control system is initially approached by assuming rigid appendages and ideal actuator dynamics. We will study later the effects of a band-limited actuator and flexibility of the two appendages. The single-axis attitude controller is designed starting from the dynamic model of the system. Therefore, the first task is to write the equations of motion. Under the above assumptions, the kinetic energy of the system is given by

$$T = \frac{1}{2} J_0 \dot{\theta}^2 + 2 \frac{1}{2} m \dot{s}^2 \tag{16.1}$$

where $s = s(t)$ is the displacement of each tip mass. Note that, due to the previous assumptions and the symmetry of the problem, the angular momentum of the system must be preserved so that the two tip masses undergo the same displacement (with opposite sign). The virtual work done by the control torque and the unwanted disturbance torque is

$$\delta W_{nc} = \delta\theta T_c + \delta\theta T_d \tag{16.2}$$

Since at this stage the flexible appendages are considered to be rigid, the displacement of each tip mass is related to the rotation of the central body by the following kinematic equation

$$s(t) = \ell\theta(t) \tag{16.3}$$

Therefore, the kinetic energy of the system is expressed as

$$\begin{aligned} T &= \frac{1}{2} J_0 \dot{\theta}^2 + 2 \frac{1}{2} m \ell^2 \dot{\theta}^2 \\ &= \frac{1}{2} \left(J_0 + 2 m \ell^2 \right) \dot{\theta}^2 \end{aligned} \tag{16.4}$$

Using the Lagrange equations, the rotational dynamics of the rigid system is governed by the following equation

$$J \ddot{\theta} = T_c + T_d \tag{16.5}$$

where

$$J = J_0 + 2 m \ell^2 \tag{16.6}$$

is the total equivalent moment of inertia of the system.

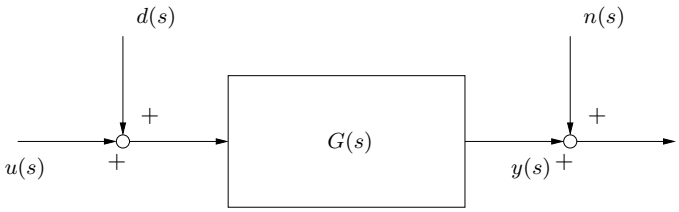

Figure 16.2 Block diagram of the open-loop system.

In the Laplace domain, the dynamic relation between the rotation $\theta(s)$ and the control and disturbance torques is written as

$$\theta(s) = \frac{1}{s^2 J} T_c(s) + \frac{1}{s^2 J} T_d(s) \tag{16.7}$$

which can be also expressed using the classical control notation as

$$y(s) = G(s)u(s) + G_d(s)d(s) \tag{16.8}$$

where y is the system output, u is the control input, d is the disturbance, $G(s)$ is the system transfer function related to the control path and $G_d(s)$ is the system transfer function of the disturbance path. Note that, in this case, $G(s) = G_d(s)$ since we have assumed the disturbance torque acting on the central body as the control torque.

Note also that the system output is typically measured with an attitude sensor which is affected by noise. The usual scheme implies that the noise $n(s)$ is added to the system output $y(s)$. We can write that the noisy measure is

$$y_n(s) = G(s)u(s) + G(s)d(s) + n(s) \tag{16.9}$$

Therefore, the block diagram for the system under investigation can be represented as in Figure 16.2. It is clear that the open-loop behaviour is unstable due to the presence of the double pole at the origin.

16.2.2 Control scheme and objectives

The goal of the present application is to design a control system such that the spacecraft is rotated by a desired angle $\theta_r = r$ (reference angle) from an initial attitude angle at time $t = t_0$. Without any loss of generality, the initial angle and time instant can be taken as zero. The above manoeuvre, corresponding to a step response of the system, must be performed within a prescribed amount of time and the closed-loop response must have limited overshoot compared to the reference angle. Furthermore, the steady-state error between the actual and reference attitude must be equal to zero.

The requirements outlined thus far can be satisfied by a properly designed feedback controller. The block diagram is reported in Figure 16.3, where $R(s)$ is the transfer function of the controller to be determined by the closed-loop design process. Generally speaking, any feedback control system should exhibit the following properties:

- closed-loop stability
- capability to follow the reference signal with prescribed static and dynamic performance
- capability of rejecting disturbance
- capability of rejecting measurement noise
- robustness against model uncertainties

Let's examine the implications of the above requirements.

Stability. The requirement on closed-loop stability implies that, when the feedback loop is closed, the system must be asymptotically stable, i.e., all the poles representing the closed-loop system dynamics lie in the left half complex plane (i.e., the real part of the closed-loop poles must be negative). We will promptly show that all the closed-loop poles are the roots of a single transfer function. Therefore, the analysis of that function will suffice in checking the stability of the system.

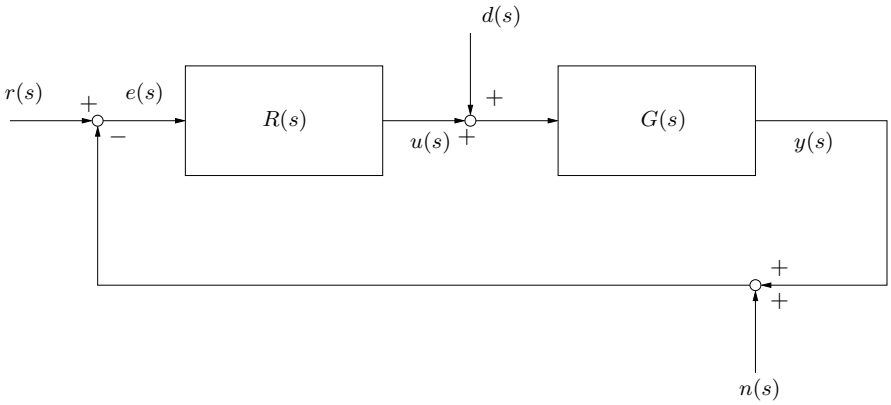

Figure 16.3 Block diagram of the closed-loop system.

Reference tracking. Tracking capabilities are generally expressed in terms of steady-state error (static property) and transient behavior (dynamic properties).

The steady-state objective is for the output to match the reference signal. That is, once the transients are died out, we would like to have

$$e(t) = r(t) - y(t) \approx 0 \quad \text{when} \quad t \to \infty \qquad \text{(steady-state requirement)} \tag{16.10}$$

In our attitude control, we require that the actual attitude eventually matches the desired attitude. It is noted that the above requirement should be achieved for any reference $r(t)$. In general, $r(t)$ may not be constant or may not be known in advance. In some cases, there are practical factors that prevent the steady-state error from going to zero. The common design rule is to evaluate the static property of the control system in terms of a few test reference signals, which typically include the step input and the ramp input. If the closed-loop static behaviour is good for the test signals, the control design is considered to be satisfactory.

More often than not, transient specifications are given with reference to a unit step command. They typically include prescribed values of the following time-domain parameters (see Figure 16.4):

- rise-time t_r (the time taken for the output to rise from 10% to 90% of the final value)
- peak-time t_p (the time taken for the output to first achieve the peak response)
- overshoot M_p (the distance between the peak response and the steady-state response)
- settling-time t_s (the time taken for the output to get to within some $\epsilon\%$ (typically 1 or 2%) of the final value and stay there)

The analyst must design a controller capable of satisfying one or more of the above requirements. We will see that transient specifications can be also expressed by frequency-domain parameters so that transient performances correspond to a prescribed shape of the frequency response of the system. Furthermore, maximum values of the above characteristic time parameters can be related to allowable regions for closed-loop poles in the complex plane. Therefore, dynamic properties of the closed-loop system can be selected by studying the root locus, which plots the locations of the closed-loop poles as a function of the gain of the controller.

Disturbance rejection. Disturbance rejection implies the capability of the closed-loop system of attaining good reference tracking when the plant is subjected to disturbing forces. This requirement involves some constraints on the shape of the system transfer function and can be typically satisfied if the frequency content of the disturbance is known.

Noise rejection. Measurement noise rejection implies the capability of the closed-loop system of attaining good reference tracking when the plant is subjected to measurement noise. Similarly to disturbance rejection, this requirement involves some constraints on the shape of the system transfer function and can be typically satisfied if the frequency content of the noise is known.

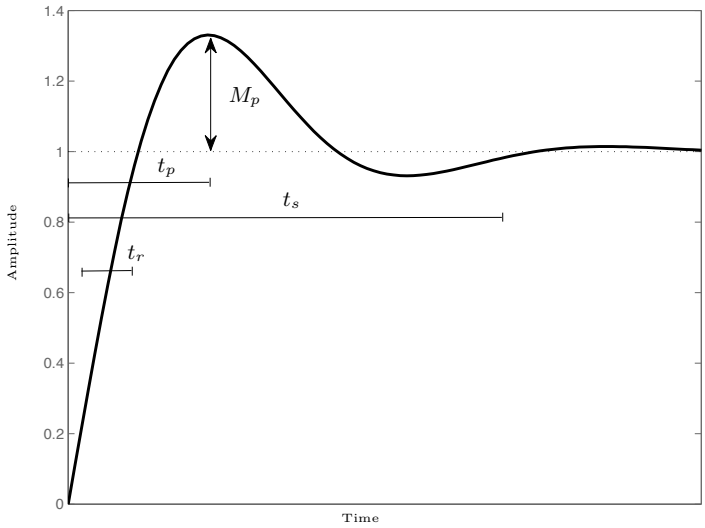

Figure 16.4 Generic step response of an underdamped second-order system with time-domain specifications.

Robustness. As a final requirement of the closed-loop system, the design of the control law must be sufficiently robust against modelling errors and/or variation of the system parameters. This means that the closed-loop stability must be ensured not only under nominal conditions but also when model uncertainties are present. Furthermore, the static and dynamic performances should not deviate much from those computed by the nominal design. Of course, closed-loop stability and performance in perturbed conditions cannot be guaranteed in advanced for *any* perturbation of the system parameters. In practice, the designer must provide a reliable estimate of the uncertainty margins of the model and perform an analysis of the closed-loop behaviour for perturbations falling within the above margins.

According to what discussed above and the scheme reported in Figure 16.3, the control law is written in the Laplace domain as

$$u(s) = R(s)e(s) \tag{16.11}$$

where

$$e(s) = r(s) - [y(s) + n(s)] \tag{16.12}$$

is the output error. Therefore, the system output is written as

$$\begin{aligned} y(s) &= G(s)R(s)e(s) + G(s)d(s) \\ &= G(s)R(s)\left[r(s) - y(s) - n(s)\right] + G(s)d(s) \\ &= \frac{R(s)G(s)}{1 + R(s)G(s)}r(s) - \frac{R(s)G(s)}{1 + R(s)G(s)}n(s) + \frac{G(s)}{1 + R(s)G(s)}d(s) \end{aligned} \tag{16.13}$$

or, alternatively,

$$y(s) = \frac{L(s)}{1 + L(s)}r(s) + \frac{G(s)}{1 + L(s)}d(s) - \frac{L(s)}{1 + L(s)}n(s) \tag{16.14}$$

where

$$L(s) = R(s)G(s) \tag{16.15}$$

is the so-called *loop transfer function*. Equation (16.14) clearly shows that the output dynamics is characterized by the following three (actually two) transfer functions:

- $\dfrac{L(s)}{1+L(s)}$, which is called complementary sensitivity function (denoted as $T(s)$)
- $\dfrac{G(s)}{1+L(s)}$, which is called disturbance sensitivity function
- $\dfrac{L(s)}{1+L(s)}$, which is called noise sensitivity function

In terms of the error between the reference and the system output, we have

$$\begin{aligned} e(s) &= r(s) - y(s) \\ &= r(s) - \frac{R(s)G(s)}{1+R(s)G(s)}r(s) + \frac{R(s)G(s)}{1+R(s)G(s)}n(s) - \frac{G(s)}{1+R(s)G(s)}d(s) \\ &= \frac{1}{1+L(s)}r(s) - \frac{G(s)}{1+L(s)}d(s) + \frac{L(s)}{1+L(s)}n(s) \end{aligned} \tag{16.16}$$

which is expressed in terms of the disturbance and noise sensitivity functions defined above and in terms of the following transfer function

- $\dfrac{1}{1+L(s)}$, which is called sensitivity function (denoted as $S(s)$)

Note that, by definition, the sensitivity and complementary sensitivity functions are related by the following equation

$$T(s) + S(s) = 1 \tag{16.17}$$

16.2.3 General design guidelines

Equations (16.14) and (16.16) represent the key relationships for the design of a feedback control system. Before proceeding with some control solutions of the specific problem under investigation, let discuss the general design guidelines to be followed in order to achieve the closed-loop requirements declared at the beginning of the previous section.

First, we must ensure the closed-loop stability of the system. As already recalled, the stability is governed by the location of the poles. It is clear from Eqs. (16.14) and (16.16) that the closed-loop poles are the roots of the following equation

$$1 + L(s) = 0 \tag{16.18}$$

which represents the common denominator of the sensitivity functions of the system. Therefore, the controller $R(s)$ must be selected such that the roots of Eq. (16.18) have negative real part.

According to tracking capability, the ideal control system would be such that the output y matches perfectly the reference r, i.e., $y = r$. This goal should be achieved along with good rejection of disturbance and measurement noise, i.e., disturbance and noise acting on the system should not significantly affect the reference tracking. To this aim, by referring to Eq. (16.14), we require that

$$\begin{aligned} &\frac{L(s)}{1+L(s)} \to 1 && \text{for reference tracking} \\ &\frac{G(s)}{1+L(s)} \to 0 && \text{for disturbance rejection} \\ &\frac{L(s)}{1+L(s)} \to 0 && \text{for noise rejection} \end{aligned} \tag{16.19}$$

By referring to Eq. (16.16), perfect tracking ($e = 0$) implies also that

$$\begin{aligned} &\frac{1}{1+L(s)} \to 0 \\ &\frac{G(s)}{1+L(s)} \to 0 \\ &\frac{L(s)}{1+L(s)} \to 0 \end{aligned} \tag{16.20}$$

It is seen that good reference tracking is possible with complementary sensitivity function $T(s) \approx 1$ and sensitivity function $S(s) \approx 0$. This is also completely compatible with relation (16.17). Furthermore, the above requirements on the sensitivity functions leads to a good disturbance rejection of the closed-loop system. Therefore, good reference tracking can be achieved along with good disturbance rejection by taking large loop function at any frequency ω which characterizes the reference and disturbance signals , i.e.,

$$|L(j\omega)| \gg 1 \qquad \text{(good reference tracking and disturbance rejection)} \tag{16.21}$$

The drawback of this choice lies in the complete lack of noise rejection capabilities. Indeed, good noise rejection is achieved by taking small values of the loop function, i.e.,

$$|L(j\omega)| \ll 1 \qquad \text{(good noise rejection)} \tag{16.22}$$

The above requirements are clearly in contrast. It means that *good tracking, disturbance rejection and noise rejection cannot be simultaneously met at all frequencies*.

Fortunately, a satisfactory design can be generally achieved since the frequency content of the reference and disturbance signal is typically well separated from the frequency content of the measurement noise. In most applications, both reference and external disturbances vary relatively slow with time, so that their characteristic frequency content is in the low frequency range. On the contrary, the noise arising from sensors typically vary rapidly with time, that is, it is characterized by high frequencies. Therefore, the design should be performed such that

$$|L(j\omega)| \gg 1 \qquad \text{over the appropriate } \textit{low frequency range} \tag{16.23}$$

and

$$|L(j\omega)| \ll 1 \qquad \text{over the appropriate } \textit{high frequency range} \tag{16.24}$$

In other words, closed-loop tracking and disturbance rejection requirements place lower-bound restrictions on the modulus of the loop function L at low frequencies, whereas measurement noise attenuation requirements place upper-bound restrictions on the modulus of the loop function in the high frequency range. An example is shown in Figure 16.5, where the shaded regions denote the low- and high-frequency restrictions discussed above. This also implies that the log-plot of the magnitude of the loop function must cross the zero-dB axis at least one time. The lowest crossing frequency is typically called gain *cross-over frequency* of the closed-loop system, which corresponds to the frequency where $|L(j\omega)| = 1$.

As a result, the sensitivity functions should behave as

$$|T(j\omega)| \approx \begin{cases} 1 & \omega \leq \omega_c \\ 0 & \omega > \omega_c \end{cases} \tag{16.25}$$

and

$$|S(j\omega)| \approx \begin{cases} 0 & \omega \leq \omega_c \\ 1 & \omega > \omega_c \end{cases} \tag{16.26}$$

where ω_c is the cross-over frequency. Therefore, the complementary sensitivity function $T(s)$ should approximate an ideal low-pass filter with corner frequency ω_c, and the sensitivity function $S(s)$ should have a corresponding high-pass filtering behavior. Since the bandwidth of a low-pass filter is determined by the corner frequency, we can say that the closed-loop bandwidth of a feedback control system can be expressed by the cross-over frequency ω_c.

The desired loop shaping of $L(s)$ discussed thus far should also provide a closed-loop system having prescribed static and dynamic properties in tracking a reference and rejecting disturbance and measurement noise.

Static requirements are typically achieved by imposing a minimum slope of $|L(s)|$ at $s = 0$. Indeed, using the final value theorem, the steady-state error can be expressed as

$$e_{\text{ss}} = \lim_{t\to\infty} e(t) = \lim_{s\to 0} se(s) \tag{16.27}$$

If we consider the effect of the reference signal on the error, the above equation is written as

$$e_{\text{ss}} = \lim_{s\to 0} \frac{s}{1 + L(s)} r(s) \tag{16.28}$$

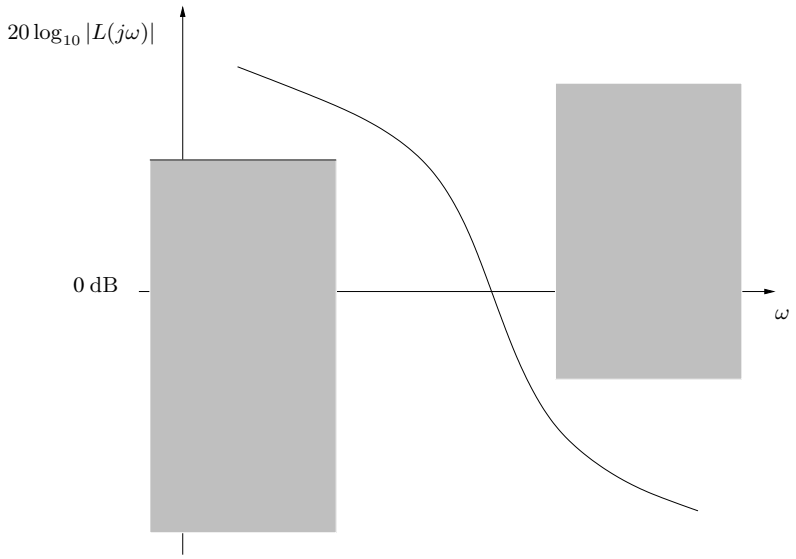

Figure 16.5 Example of desired shape of magnitude of the loop transfer function $|L(j\omega)|$.

Let us now examine two common cases. The first involves a step reference signal, i.e., $r(s) = 1/s$. Therefore, we can write the steady-state error as

$$e_{\text{ss}} = \lim_{s\to 0} \frac{s}{1+L(s)} \frac{1}{s} = \lim_{s\to 0} \frac{1}{1+L(s)} = \frac{1}{1+\lim_{s\to 0} L(s)} \tag{16.29}$$

The loop transfer function can be expressed in general as follows

$$L(s) = \frac{g}{s^N} \frac{\prod_{i=1}^{m}(s-z_i)}{\prod_{i=1}^{n}(s-p_i)} \tag{16.30}$$

with m zeros z_i, n non-zero poles p_i, and N poles at $s = 0$. The value N specifies the type of the system. For example, a type-0 system has $N = 0$, a type-1 system has $N = 1$, and so on. Note that it corresponds to the slope of the magnitude of $L(s)$ near the origin. For our purposes, it is better to rearrange Eq. (16.30) to yield

$$L(s) = \frac{\bar{g}}{s^N} \frac{\prod_{i=1}^{m}(1+sT_{zi})}{\prod_{i=1}^{n}(1+sT_{pi})} \tag{16.31}$$

where

$$\bar{g} = g \frac{\prod_{i=1}^{m}(-z_i)}{\prod_{i=1}^{n}(-p_i)} \tag{16.32}$$

and

$$T_{zi} = -\frac{1}{z_i} \qquad T_{pi} = -\frac{1}{p_i} \tag{16.33}$$

Comparing Eq. (16.29) and Eq. (16.31) we can draw the following conclusions on the static performance of the closed-loop system for a step reference:

- A type-0 system has a non-null steady-state error given by

$$e_{\rm ss} = \frac{1}{1+\bar{g}} \tag{16.34}$$

- A type-N system with $N \geq 1$ has zero steady-state error.

The second case under investigation involves a ramp reference signal, i.e., $r(s) = 1/s^2$. The steady-state error is given by

$$e_{\rm ss} = \lim_{s\to 0} \frac{s}{1+L(s)} \frac{1}{s^2} = \lim_{s\to 0} \frac{1}{s+sL(s)} = \lim_{s\to 0} \frac{1}{sL(s)} \tag{16.35}$$

Using the results derived for a step reference, we can conclude that

- A type-0 system has a non-zero steady-state error given by

$$e_{\rm ss} = \lim_{s\to 0} \frac{1}{s\bar{g}} = \infty \tag{16.36}$$

  which shows that a type-0 system cannot track a ramp input.

- A type-1 system has a non-zero steady-state error given by

$$e_{\rm ss} = \lim_{s\to 0} \frac{1}{s\dfrac{\bar{g}}{s}} = \frac{1}{\bar{g}} \tag{16.37}$$

- A type-N system with $N \geq 2$ has zero steady-state error with respect to a ramp reference.

We could go on by studying reference inputs of higher order. However, the general trend can be already envisaged from the two cases considered above. Indeed, the static properties of a closed-loop system with respect to a reference input are good if the loop transfer function contains a prescribed number of poles at the origin. Such number can be selected by adding integrators in the controller function $R(s)$. The minimum number of poles at the origin is related to the type of reference (step, ramp, ...). In general, the more integrators in the loop, the higher the order of reference signal that can be tracked.

In some cases, the closed-loop system must also provide static requirements with respect to the disturbance. In practice, the nature of disturbances is unknown. However, if the disturbance is slowly varying with time, a constant disturbance can be taken as a good approximation for the purpose of initial controller design. Let us examine the effect of a constant disturbance of amplitude $\bar{T}_d$ on the steady-state error of the closed-loop system. According to Eq. (16.16), the error is related to the disturbance by the following equation

$$e(s) = -\frac{G(s)}{1+L(s)} d(s) \tag{16.38}$$

Using the final-value theorem, the corresponding steady-state value for a constant disturbance is given by

$$e_{\rm ss} = \lim_{s\to 0} \frac{sG(s)}{1+L(s)} \frac{\bar{T}_d}{s} = \lim_{s\to 0} \frac{G(s)}{1+L(s)} \bar{T}_d = \lim_{s\to 0} \frac{G(s)}{1+R(s)G(s)} \bar{T}_d \tag{16.39}$$

Similarly to what done previously, the system and controller transfer functions can be expressed as

$$G(s) = \frac{k_G}{s^{N_G}} \frac{\displaystyle\prod_{i=1}^{m}(1+sT_{zGi})}{\displaystyle\prod_{i=1}^{n}(1+sT_{pGi})} \tag{16.40}$$

$$R(s) = \frac{k_R}{s^{N_R}} \frac{\prod_{i=1}^{m}(1 + sT_{zRi})}{\prod_{i=1}^{n}(1 + sT_{pRi})} \tag{16.41}$$

where k_G and k_R are the static gains of the system and the controller, respectively, N_G and N_R are the system and controller type, and T_z and T_p are the reciprocals of zeros and poles of the two functions. The above relations can be also written more compactly as

$$G(s) = \frac{k_G}{s^{N_G}} \frac{N_G(s)}{D_G(s)} \tag{16.42}$$

and

$$R(s) = \frac{k_R}{s^{N_R}} \frac{N_R(s)}{D_R(s)} \tag{16.43}$$

Therefore, the steady-state error to a step disturbance is

$$e_{\text{ss}} = \lim_{s \to 0} \frac{s^{N_R} k_G N_G(s) D_R(s)}{s^{N_G + N_R} D_G(s) D_R(s) + k_G k_R N_R(s) N_G(s)} \bar{T}_d \tag{16.44}$$

One can easily see that, in order to have a zero steady-state error of the closed-loop system due to a step disturbance, the controller $R(s)$ must be at least of type 1, i.e., $N_R \geq 1$. That is, there must be an integrator $1/s$ in the controller to reject a constant disturbance.

As already outlined, dynamic performance of the closed-loop system can be specified in different ways. Often, dynamic requirements are expressed in terms of time-domain specifications. It is also possible to recast some time-domain specifications as frequency-domain specifications, and therefore find a correspondence between closed-loop transient characteristics and shaping of the loop function $L(s)$. Even if for complex systems it is very difficult to establish such exact correspondence, we can use the results obtained for simple systems as guidelines to design $L(s)$ in practical applications.

An example of the correspondence between time-domain and frequency-domain specifications is related to the speed of the closed-loop response of the system. If we consider the common test case of a step reference input, the speed of the response can be expressed by the rise-time and settling-time. It can be shown that, in some simple cases, the above time-domain parameters can be explicitly related to the gain cross-over frequency of the closed-loop system. Therefore, a prescribed rise- and settling-time can be specified by designing a loop function $L(s)$ with prescribed bandwidth. Indeed, it is known that the larger the bandwidth of a system, the higher the speed of the response to an input. This can be considered as a general guideline which can be used also for those systems whose complexity prevents to find an explicit relationship between rise-time and bandwidth.

Another example of correspondence between time- and frequency-domain properties of the control system involves the maximum overshoot of the closed-loop response, which is again typically related to a unit step command. The overshoot is a property which can be computed from the time response and is strongly dependent on the damping ratio of the closed-loop system. It can be shown that the damping, and so the maximum overshoot, is related to the *phase margin* of the system, i.e., a prescribed maximum overshoot can be recast as a prescribed system phase margin. The phase margin is defined as how much phase lag can be added to the open-loop system without making it unstable. It can be calculated as the angle by which the phase of $L(s)$ is short of -180^o when the magnitude of $L(s)$ is unity, which corresponds to the cross-over frequency ω_c. A companion quantity is the so called *gain margin*, which is defined as the amount by which the gain can be increased before the system becomes unstable. It has the value $1/x$, where x is the magnitude of $L(s)$ corresponding to a phase of -180^o, and it is normally quoted in decibels. Gain and phase margin can be read off directly from the Bode plot of the loop function $L(s)$ as shown in Figure 16.6. To determine the phase margin, find the frequency at which the magnitude is unity (or 0 dB for a log-plot), read off the phase and note by how many degrees it is above the -180^o level. To determine the gain margin, find the frequency for which the phase is -180^o, read off the magnitude for this frequency and note how many dB this is below zero.

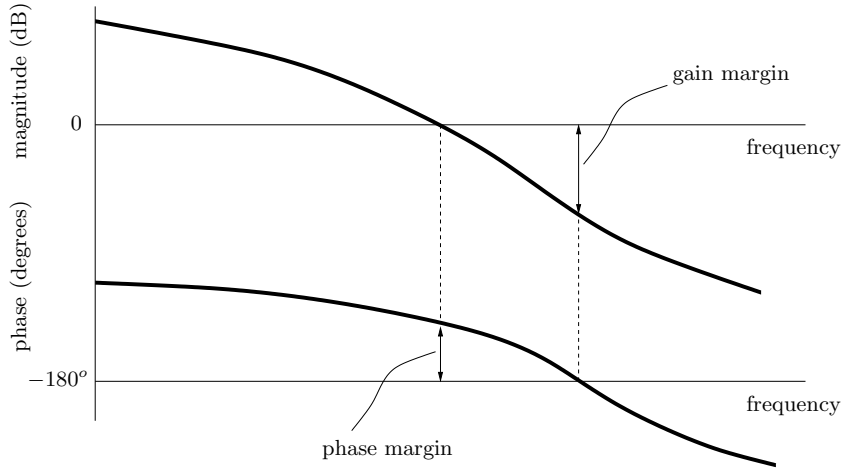

Figure 16.6 Example of computation of gain and phase margins of $L(s)$.

16.2.4 Closed-loop requirements

After the brief discussion on general guidelines for the design of feedback control systems presented thus far, let now return to the satellite example under investigation to apply some of the outlined considerations. The following analysis is supported by numerical solutions based on the following data:

- $J_0 = 0.9$ kg m^2
- $m = 0.5$ kg
- $\ell = 1$ m

Therefore, the total equivalent moment of inertia of the rigid system is $J = 1$ kg m^2. According to the scheme in Figure 16.3, we must design a controller $R(s)$ so that the closed-loop system is stable and satisfies the following specifications for a unit step reference:

1. Steady-state error must be zero
2. Rise-time $t_r \leq 30$ s
3. Maximum overshoot percentage $M_p\% \leq 30$ %
4. Settling-time $t_s \leq 100$ s

Moreover, we require that

5. Steady-state error for a step disturbance must be zero
6. High-frequency decay rate of -40 dB/decade for good noise rejection

16.2.5 Proportional (P) control

The simplest solution we can imagine for the attitude control of our satellite is the so-called proportional control (P-control). It is based on the following control law

$$u(t) = k_p e(t) \tag{16.45}$$

where k_p is a positive coefficient called the proportional gain. The above relationship can be written in the Laplace domain as

$$u(s) = k_p e(s) \tag{16.46}$$

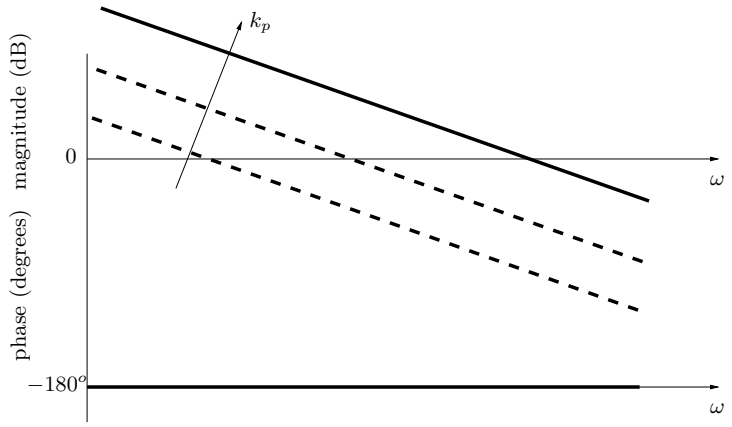

Figure 16.7 Bode plot (magnitude and phase) of $L(s)$ with a P-control.

The resulting loop function is

$$L(s) = R(s)G(s) = \frac{k_p}{Js^2} \tag{16.47}$$

which corresponds to the following complementary sensitivity function

$$T(s) = \frac{L(s)}{1 + L(s)} = \frac{k_p}{Js^2 + k_p} \tag{16.48}$$

and disturbance sensitivity function

$$\frac{G(s)}{1 + L(s)} = \frac{1}{Js^2 + k_p} \tag{16.49}$$

Therefore, the loop function is a double-integrator system as the open-loop behaviour with a different gain due to the presence of the coefficient k_p. As such, the phase of $L(s)$ is equal to -180^o.

The P-control is completely unsatisfactory for this application. This can clearly seen by writing the closed-loop equation of motion

$$J\ddot{\theta} = k_p\left(\theta_r - \theta\right) + T_d \tag{16.50}$$

or, alternatively,

$$J\ddot{\theta} + k_p\theta = k_p\theta_r + T_d \tag{16.51}$$

which corresponds to an undamped oscillatory attitude motion.

Indeed, the closed-loop poles are purely imaginary and are given by

$$s_{1,2} = \pm j\sqrt{\frac{k_p}{J}} \tag{16.52}$$

Therefore, by increasing k_p, the system becomes stiffer and stiffer since the bandwidth enlarges as shown in the Bode plot of $L(s)$ in Figure 16.7. However, since the P-control involves only a static action, the phase is unchanged and the phase margin is equal to zero.

In terms of the root locus, the poles move from the origin along the imaginary axis, which represents the asymptote location in this case (see Figure 16.8). However, using a single proportional gain no damping is added to the system (the closed-loop poles do not move to the left of the imaginary axis) and the asymptotic stability is missed. As a result, closed-loop specifications cannot be met.

16.2.6 Proportional-derivative (PD) control

A significant improvement with respect to the simple P-control is achieved if we also include a derivative control action. The resulting controller is called proportional-derivative control (PD-control). The feedback control law can be

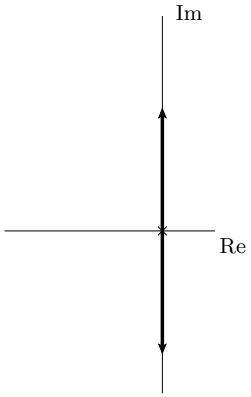

Figure 16.8 Effect of a P-control on root locus.

implemented as follows

$$u(t) = k_p e(t) + k_d \dot{e}(t) \tag{16.53}$$

where the first term is related to the proportional action and the second term to the derivative action. The proportional control is governed by the proportional gain k_p, whereas the derivative control is governed by the derivative gain k_d. The overall control action will result from the contribution of both terms. We anticipate that, since the control law now includes a term proportional to the time-derivative of the error, we can add some damping to the system. This can be argued by looking at the closed-loop equation of motion, which is given by

$$J\ddot{\theta} + k_d\dot{\theta} + k_p\theta = k_p\theta_r + T_d \tag{16.54}$$

It clearly corresponds to a damped oscillatory attitude motion.

The PD-control law may be written in the Laplace domain as

$$u(s) = (k_p + sk_d)\, e(s) \tag{16.55}$$

Therefore, the transfer function of the controller is

$$R(s) = k_p + sk_d \tag{16.56}$$

and the control design is based on the loop function

$$L(s) = R(s)G(s) = \frac{k_p + sk_d}{Js^2} \tag{16.57}$$

Using the numerical values of the problem, we can write

$$L(s) = \frac{k_p + sk_d}{s^2} \tag{16.58}$$

Let now examine the design procedure to satisfy the closed-loop specifications. The first requirement is to have zero steady-state error for a unit step reference. In our case we can write

$$e_{\text{ss}} = \frac{1}{1 + \lim\limits_{s\to 0} L(s)} = \frac{1}{1 + \lim\limits_{s\to 0} \dfrac{k_p + sk_d}{s^2}} = \frac{1}{1+\infty} = 0 \tag{16.59}$$

irrespective of the value of k_p and k_d. Therefore, the first specification is satisfied by the PD-control.

The control system must also provide some dynamic performance which are specified as time-domain characteristics of the closed-loop system response. The relationship between the output and the reference is expressed by the complementary sensitivity function, which is given by

$$T(s) = \frac{k_p + sk_d}{Js^2 + sk_d + k_p} \tag{16.60}$$

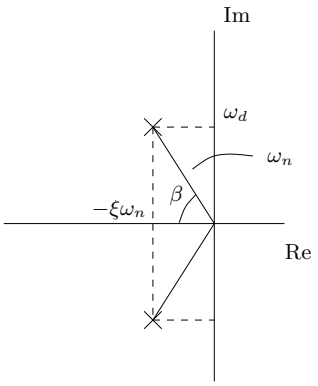

Figure 16.9 Pole location of a PD-control.

The complementary sensitivity function in Eq. (16.60) can be also written in an alternative form as follows

$$T(s) = \frac{2\xi\omega_n s + \omega_n^2}{s^2 + 2\xi\omega_n s + \omega_n^2} \tag{16.61}$$

where

$$\begin{aligned} \frac{k_p}{J} &= \omega_n^2 \\ \frac{k_d}{J} &= 2\xi\omega_n \end{aligned} \tag{16.62}$$

Since in our case $J = 1$, we have $k_p = \omega_n^2$ and $k_d = 2\xi\omega_n$. The quantity ω_n can be considered as the natural frequency of the closed-loop system and ξ is the corresponding damping ratio. It can be seen that the closed-loop transfer function has one real zero at

$$z = -\frac{\omega_n}{2\xi} \tag{16.63}$$

and two closed-loop poles at

$$p_{1,2} = -\xi\omega_n \pm \omega_n\sqrt{\xi^2 - 1} \tag{16.64}$$

Since the desired damping ratio is typically less than one, the poles are complex conjugate and can be expressed as

$$p_{1,2} = -\xi\omega_n \pm j\omega_n\sqrt{1 - \xi^2} \tag{16.65}$$

or, alternatively,

$$p_{1,2} = -\xi\omega_n \pm j\omega_d \tag{16.66}$$

where $\omega_d = \omega_n\sqrt{1 - \xi^2}$ is the damped natural frequency. The poles have negative real part provided that k_p and k_d are real and positive coefficients. This is the required condition for closed-loop stability. It is also worth noting that the natural frequency of the system is dependent on the proportional gain k_p, whereas the damping is governed by the derivative gain k_d. Therefore, by adjusting the two gains, we can provide a fast response with a limited overshoot. This is almost equivalent of selecting the locations of the closed-loop poles in Eq. (16.65), which are shown in Figure 16.9.

In order to find the gain values which satisfy the transient specifications of the problem, let consider the closed-loop response to a step reference input. In this case, $r(s) = 1/s$. According to what derived above, the system output is given in the Laplace domain by

$$y(s) = \frac{1}{s}\frac{2\xi\omega_n s + \omega_n^2}{s^2 + 2\xi\omega_n s + \omega_n^2} \tag{16.67}$$

Note that the above equation can be rearranges as follows

$$\begin{aligned} y(s) &= \frac{1}{s} - \frac{s}{s^2 + 2\xi\omega_n s + \omega_n^2} \\ &= \frac{1}{s} - \frac{s + \xi\omega_n - \xi\omega_n}{s^2 + 2\xi\omega_n s + \xi^2\omega_n^2 + \omega_n^2 - \xi^2\omega_n^2} \\ &= \frac{1}{s} - \frac{s + \xi\omega_n}{(s + \xi\omega_n)^2 + \omega_d^2} + \frac{\xi\omega_n}{\omega_d}\frac{\omega_d}{(s + \xi\omega_n)^2 + \omega_d^2} \end{aligned} \tag{16.68}$$

Taking the inverse Laplace transform, we obtain the step response to a unit reference in the time domain as

$$y(t) = 1 - e^{-\xi\omega_n t}\left[\cos(\omega_d t) - \frac{\xi\omega_n}{\omega_d}\sin(\omega_d t)\right] \tag{16.69}$$

This equation can be studied to determine the gains of the PD-control.

First, note that the asymptotic value of $y(t)$ for $t \to \infty$ is one, as expected from the previous analysis of the static properties. Equation (16.69) also shows that the frequency of oscillation is ω_d and the rate of decay is $\xi\omega_n$.

Let's compute the peak-time of the step response. It occurs at the first time when $dy/dt = 0$. The derivative of Eq. (16.69) is given by

$$\frac{dy}{dt} = e^{-\xi\omega_n t}\sin(\omega_d t)\left[\frac{\xi^2\omega_n^2}{\omega_d} + \omega_d\right] \tag{16.70}$$

It is equal to zero when

$$\omega_d t = n\pi \tag{16.71}$$

where n is a positive integer. $n = 0$ corresponds to the initial time $t = 0$. The peak-time t_p occurs when $n = 1$ and it is given by

$$t_p = \frac{\pi}{\omega_d} \tag{16.72}$$

A prescribed fast response of the system can be obtained by imposing a maximum value of the peak-time $t_p^{\max}$ and selecting the controller gains such that $t_p \leq t_p^{\max}$. From Eq. (16.72) it is clear that the above requirement is satisfied if

$$\frac{\pi}{\omega_d} \leq t_p^{\max} \tag{16.73}$$

which corresponds to a minimum value of the damped frequency ω_d such that

$$\omega_d \geq \frac{\pi}{t_p^{\max}} \tag{16.74}$$

Since for an underdamped system the peak-time is always larger than the rise-time, selecting $t_p^{\max} = 30$ s allows satisfying the requirement on the rise-time of the closed-loop response. In our numerical case, we have

$$\omega_d \geq \frac{\pi}{30} \approx 0.105 \tag{16.75}$$

Since ω_d is the imaginary part of the closed-loop poles (see Eq. (16.66)), we can identify a region in the complex plane where the poles should lie in order to meet the above specification. The allowable region of poles location for the rise-time constraint is approximately the non-shaded region in Figure 16.10.

Note that, in some cases, the constraint equation (16.74) can be too restrictive. Indeed, imposing the satisfaction of the rise-time specification by using Eq. (16.73), which actually involves the peak-time parameter, may lead to an excessive control action which must be compatible with the actuator limitations in terms of the maximum amount of torque it can apply. However, the procedure outlined thus far can be considered as a good approximation for the initial design, which can be refined by trial-and-error.

Using what derived for the peak-time, we can find a constraint equation on the minimum damping value of the closed-loop response in order to satisfy the overshoot specification. The maximum response occurs at the peak-time t_p. It is

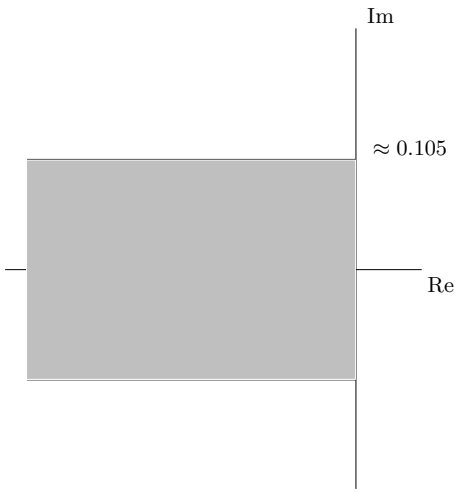

Figure 16.10 Allowable region for peak-time constraint.

given by

$$\begin{aligned} y_p = y(t_p) &= 1 - e^{-\xi\omega_n t_p}\left[\cos(\omega_d t_p) - \frac{\xi\omega_n}{\omega_d}\sin(\omega_d t_p)\right] \\ &= 1 - e^{-\frac{\pi\xi\omega_n}{\omega_d}}\left[\cos\pi - \frac{\xi\omega_n}{\omega_d}\sin\pi\right] \\ &= 1 + e^{-\frac{\pi\xi}{\sqrt{1-\xi^2}}} \end{aligned} \tag{16.76}$$

which shows that it depends only on the damping ratio ξ. The overshoot is then

$$M_p = y_p - 1 = e^{-\frac{\pi\xi}{\sqrt{1-\xi^2}}} \tag{16.77}$$

and the percentage value is

$$M_p\% = e^{-\frac{\pi\xi}{\sqrt{1-\xi^2}}} \times 100\% \tag{16.78}$$

The maximum overshoot specification is recast into the following constraint equation involving the damping ratio

$$e^{-\frac{\pi\xi}{\sqrt{1-\xi^2}}} \leq M_p^{\max} \tag{16.79}$$

In our numerical study, we have $M_p^{\max} = 0.3$ and so we should enforce that

$$e^{-\frac{\pi\xi}{\sqrt{1-\xi^2}}} \leq 0.3 \tag{16.80}$$

which can be arranged as

$$\frac{\xi}{\sqrt{1-\xi^2}} \geq -\frac{\ln 0.3}{\pi} \tag{16.81}$$

or, alternatively,

$$\frac{\sqrt{1-\xi^2}}{\xi} \leq -\frac{\pi}{\ln 0.3} \tag{16.82}$$

Referring back to Figure 16.9, we can see that

$$\tan\beta = \frac{\omega_d}{\xi\omega_n} = \frac{\sqrt{1-\xi^2}}{\xi} \tag{16.83}$$

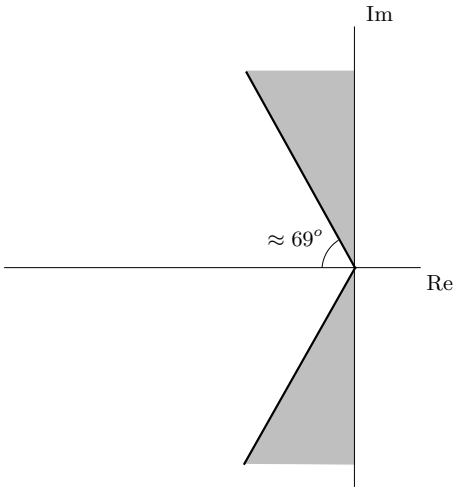

Figure 16.11 Allowable region for overshoot constraint.

Therefore, the specification on the maximum overshoot can be satisfied by imposing a maximum value of the angle β such that

$$\beta \leq \tan^{-1}\left(-\frac{\pi}{\ln 0.3}\right) \approx 69^o \tag{16.84}$$

The allowable region of poles location for the overshoot constraint is represented by the non-shaded region in Figure 16.11.

The last requirement on the transient properties of the closed-loop system involves the settling-time t_s. A conservative estimate of the settling-time can be computed by taking the time for the amplitude of the decaying sinusoid in Eq. (16.69) to reach $\epsilon\%$. If we consider the case of $\epsilon = 2$, we can write

$$\frac{e^{-\xi\omega_n t}}{\sqrt{1-\xi^2}} = 0.02 \tag{16.85}$$

Therefore, the settling-time is approximately given by

$$t_s = \frac{-\ln\left(0.02\sqrt{1-\xi^2}\right)}{\xi\omega_n} \tag{16.86}$$

For underdamped systems, the numerator of the previous equation varies between 3.9 and 4.8 for damping ratios between 0.1 and 0.9. A further approximation of the settling-time is to take the mean value of the above quantity as follows

$$t_s \approx \frac{4.4}{\xi\omega_n} \tag{16.87}$$

which shows that t_s is primarily dependent on the real part of the poles. In our problem, we should enforce that

$$\frac{4.4}{\xi\omega_n} \leq t_s^{\max} = 100 \tag{16.88}$$

which can be rearranged to give

$$\xi\omega_n \geq \frac{4.4}{100} = 0.044 \tag{16.89}$$

The allowable region of poles location for the settling-time constraint is represented by the non-shaded region in Figure 16.12.

Once we have found the allowable closed-loop pole regions for each of the individual requirements, we can combine them to find the allowable closed-loop pole region for all the dynamic specifications of the problem. This region can

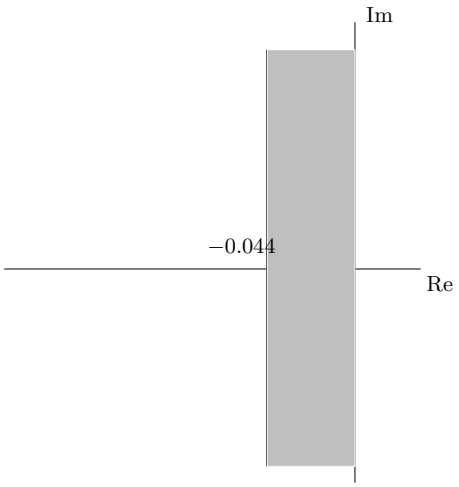

Figure 16.12 Allowable region for settling-time constraint.

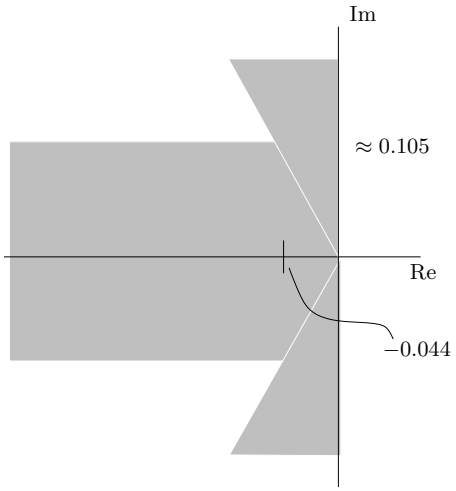

Figure 16.13 Allowable region for combined peak-time (rise-time), overshoot and settling-time constraints.

be easily determined as the intersection of the individual allowable regions, as shown in Figure 16.13. We are free to place the closed-loop poles anywhere in the non-shaded region so that prescribed transient properties of the system could be satisfied. Note that, as already mentioned, the exact satisfaction of the closed-loop specifications is not assured by the previous analysis due to the approximations we have introduced to determine the allowable pole regions. Note also that the closed-loop transfer function Eq. (16.61) contains one real zero. This means that the transient characteristics of the system are not dependent only on the location of the closed-loop poles but also on the value of the closed-loop zero. Indeed, the selection of the closed-loop complex poles, which is obtained by prescribing the real part $-\xi\omega_n$ and the imaginary part ω_d, has a direct effect on the location of the zero.

According to the previous analysis, we can impose for example that the desired closed-loop poles are

$$p_{1,2} = -0.05 \pm j0.11 \tag{16.90}$$

As outlined so far, the above choice can be considered as an initial trial of the design procedure. The final design may result from an iterative tuning process where the solution in Eq. (16.90) is taken as a reasonable starting guess. With the

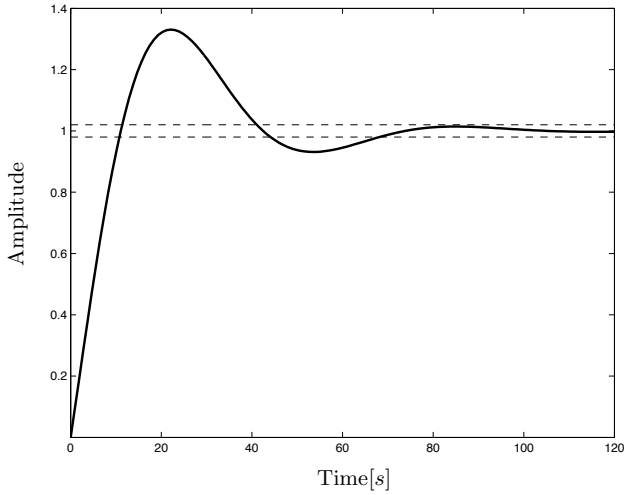

Figure 16.14 Closed-loop response to a unit step reference with a PD-control ($k_p = 0.0146$ and $k_d = 0.1$).

poles of Eq. (16.90), we can compute ω_n^2 as

$$\begin{aligned} \omega_n^2 &= \xi^2\omega_n^2 + \omega_d^2 = \xi^2\omega_n^2 + \omega_n^2\left(1-\xi^2\right) \\ &= \mathrm{Re}(p)^2 + \mathrm{Im}(p)^2 = 0.05^2 + 0.11^2 \\ &= 0.0146 \end{aligned} \tag{16.91}$$

From Eq. (16.62), we can determine the controller gains as

$$\begin{aligned} k_p &= J\omega_n^2 = \omega_n^2 = 0.0146 \\ k_d &= J2\xi\omega_n = 2\xi\omega_n = 2 \times 0.05 = 0.1 \end{aligned} \tag{16.92}$$

The corresponding transfer function of the controller takes the form

$$R(s) = 0.0146 + 0.1s \tag{16.93}$$

and the response to a unit step reference is plotted in Figure 16.14. It can be seen that the rise-time and settling-time specifications are largely met. However, the maximum percentage overshoot is slightly higher than the prescribed 30%. This is mainly due to the effect of the zero in the closed-loop transfer function.

Since the overshoot is primarily dependent on the damping ratio, we could increase the derivative action by slightly increasing the corresponding derivative gain k_d. Let's try with this choice

$$\begin{aligned} k_p &= 0.0146 \\ k_d &= 0.12 \end{aligned} \tag{16.94}$$

The corresponding step response is plotted in Figure 16.15, which shows that now the overshoot specification is met, without changing significantly the rise and settling-time of the response. The above choice corresponds approximately to the following closed-loop poles

$$p_{1,2} = -0.06 \pm j0.105 \tag{16.95}$$

It is worth noting that the present design must also deal with actuator limitations, which are not explicitly taken into account in the previous numerical analysis. This requirement has been implicitly considered by placing the closed-loop poles not too far from the origin, i.e., limiting their modulus ω_n^2 to the minimum value so that the closed-loop specifications can be met. Indeed, as a general rule, the required control action is related to the distance between open-

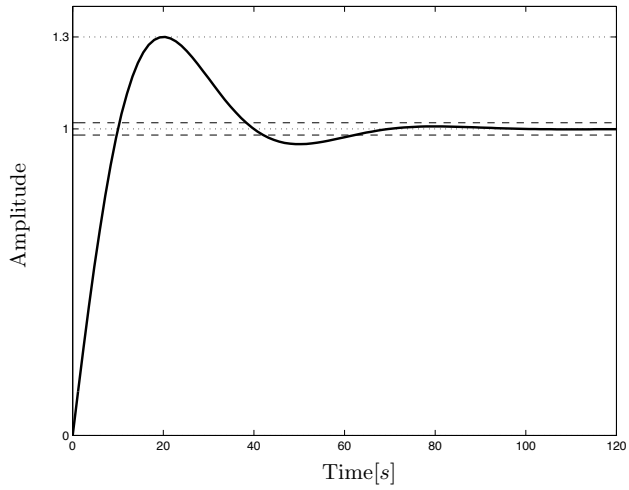

Figure 16.15 Closed-loop response to a unit step reference with a PD-control ($k_p = 0.0146$ and $k_d = 0.12$).

and closed-loop pole locations. In practical applications, the limitations of the actuator power must be carefully checked by ensuring that the control law will not demand more power than the actuator is capable of.

The PD-control can be also designed in the frequency domain by recasting the time-domain specifications into frequency-domain constraints. Using what introduced before, the loop transfer function with a PD-control can be written as

$$L(s) = \frac{k_p + sk_d}{Js^2} = \frac{2\xi\omega_n s + \omega_n^2}{s^2} \tag{16.96}$$

By putting $s = j\omega$, the following loop frequency response is obtained

$$L(j\omega) = -\frac{2j\xi\omega_n\omega + \omega_n^2}{\omega^2} = -\left(\frac{\omega_n}{\omega}\right)^2 - j2\xi\left(\frac{\omega_n}{\omega}\right) \tag{16.97}$$

The modulus and phase of the loop frequency response are given, respectively, by

$$|L(j\omega)| = \sqrt{\left(\frac{\omega_n}{\omega}\right)^4 + 4\xi^2\left(\frac{\omega_n}{\omega}\right)^2} \tag{16.98}$$

and

$$\begin{aligned} \angle L(j\omega) &= \angle\left(2j\xi\omega_n\omega + \omega_n^2\right)\left(-\frac{1}{\omega^2}\right) \\ &= \angle\omega_n^2\left(2j\xi\frac{\omega}{\omega_n} + 1\right) + \angle\left(-\frac{1}{\omega^2}\right) \\ &= \angle\omega_n^2 + \angle\left(1 + 2j\xi\frac{\omega}{\omega_n}\right) - \angle\omega^2 \\ &= \tan^{-1}\left(\frac{2\xi\omega}{\omega_n}\right) - 180^o \end{aligned} \tag{16.99}$$

Since ω_n and ξ are positive values, the expression of the phase angle shows that the phase lies in the range from -180^o to -90^o.

By definition, the cross-over frequency is found when $|L(j\omega)| = 1$, which yields

$$\left(\frac{\omega_n}{\omega}\right)^4 + 4\xi^2\left(\frac{\omega_n}{\omega}\right)^2 = 1 \tag{16.100}$$

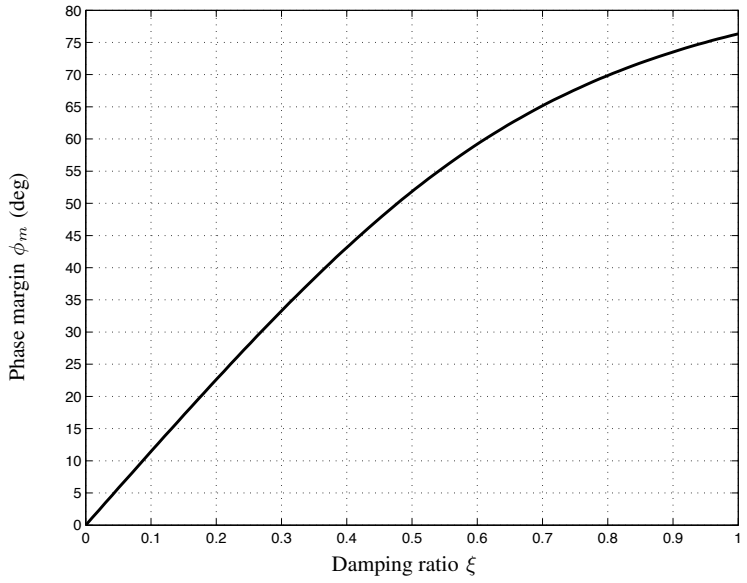

Figure 16.16 Relationship between phase margin and damping ratio expressed in Eq. (16.102).

whose (positive) solution is

$$\omega_c = \frac{\omega_n}{\sqrt{\sqrt{4\xi^4+1}-2\xi^2}} \tag{16.101}$$

The corresponding phase margin is given by

$$\phi_m = 180^o + \angle L(j\omega_c) = \tan^{-1}\left(\frac{2\xi}{\sqrt{\sqrt{4\xi^4+1}-2\xi^2}}\right) \tag{16.102}$$

where it is clear that it depends only on the damping ratio ξ. The relationship is represented in Figure 16.16. We have already found that the overshoot M_p is also dependent only on the damping ratio. As a consequence, we can relate the phase margin to the overshoot of the system response. The result is the graph in Figure 16.17. Therefore, one can find from Fig. 16.17 the required phase margin to satisfy a time-domain specification on the maximum percentage overshoot of the closed-loop response to a unit step reference. With this value, the corresponding damping ratio $\hat{\xi}$ is determined from the plot in Fig. 16.16.

Once the damping ratio $\hat{\xi}$ is specified, it is clear from Eq. (16.101) that the cross-over frequency will result from the value of the natural frequency ω_n. Recalling the constraint equations for the rise- and settling-time (2%) time, we can write

$$\omega_n \geq \frac{\pi}{t_p^{\max}\sqrt{1-\hat{\xi}^2}} \tag{16.103}$$

and

$$\omega_n \geq \frac{-\ln\left(0.02\sqrt{1-\hat{\xi}^2}\right)}{t_s^{\max}\hat{\xi}} \tag{16.104}$$

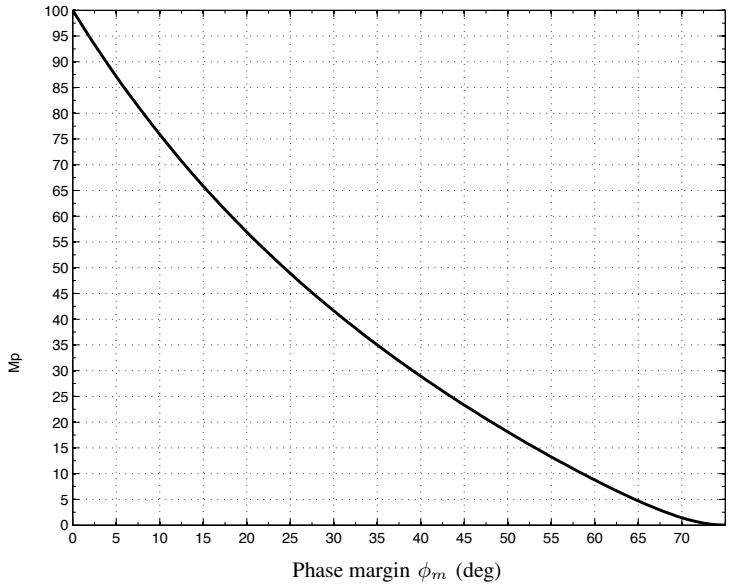

Figure 16.17 Relationship between phase margin and maximum percentage overshoot.

The last two relationships can be recast in terms of cross-over frequency. The time-domain specification on the maximum rise-time (actually, peak-time) is re-written as the following frequency-domain specification on the cross-over frequency

$$\omega_c \geq \frac{\pi}{t_p^{\max}\sqrt{\left(1-\hat{\xi}^2\right)\left(\sqrt{4\hat{\xi}^4+1}-2\hat{\xi}^2\right)}} \tag{16.105}$$

The time-domain specification on the maximum settling-time is re-written as the following frequency-domain specification on the cross-over frequency

$$\omega_c \geq \frac{-\ln\left(0.02\sqrt{1-\hat{\xi}^2}\right)}{t_s^{\max}\hat{\xi}\sqrt{\sqrt{4\hat{\xi}^4+1}-2\hat{\xi}^2}} \tag{16.106}$$

If both specifications must be met, the cross-over frequency will be selected as the highest value between Eq. (16.105) and Eq. (16.106).

Referring the previous equations to our numerical example, we should enforce a maximum percentage overshoot of 30%. This corresponds in Figure 16.17 to a phase margin of approximately 38^o. Let us choose

$$\phi_m = 40^o \tag{16.107}$$

From Fig. 16.16, this choice results in a damping ratio of approximately

$$\hat{\xi} = 0.4 \tag{16.108}$$

Using inequality (16.105), we find that the rise-time constraint $t_r \leq 30$ s should be satisfied if

$$\omega_c \geq 0.1337 \text{ rad/s} \tag{16.109}$$

Similarly, using inequality (16.106), the constraint on the maximum settling-time $t_s^{\max} = 100$ s is recast on the following cross-over specification

$$\omega_c \geq 0.1170 \text{ rad/s} \tag{16.110}$$

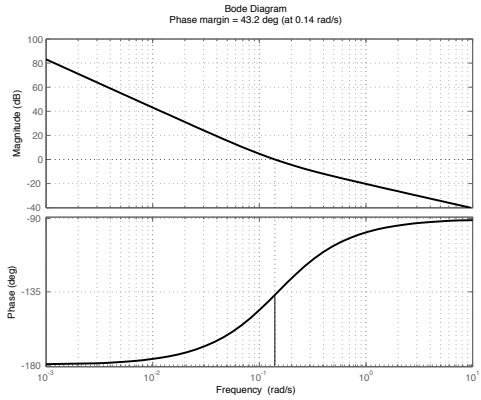

Figure 16.18 Bode diagram (magnitude and phase) of $L(s)$ with a PD-control with $k_p = 0.0143$ and $k_d = 0.0957$.

Let us choose

$$\omega_c = 0.14 \text{ rad/s} \tag{16.111}$$

This value corresponds to a natural frequency

$$\omega_n = \omega_c \sqrt{\sqrt{4\hat{\xi}^4 + 1} - 2\hat{\xi}^2} = 0.1196 \tag{16.112}$$

Therefore, the controller gains are given by

$$\begin{aligned} k_p &= \omega_n^2 = 0.0143 \\ k_d &= 2\xi\omega_n = 0.0957 \end{aligned} \tag{16.113}$$

As before, this solution can be used as a starting guess for a fine tuning of the controller. The Bode plot of $L(s)$ is reported in Figure 16.18. It is clear the phase lead introduced by the zero at

$$z = \frac{\omega_n}{2\hat{\xi}} = \frac{0.1196}{0.8} = 0.1495 \text{ rad/s} \tag{16.114}$$

The closed-loop response to a unit step reference is plotted in Figure 16.19. It is observed that the percentage overshoot is about 36%, so that the corresponding specification is not met. This is due to the value of damping.

Let's try to redesign the controller such that the phase margin is about 50^o, i.e.,

$$\phi_m = 50^o \tag{16.115}$$

With the help of Figure 16.16, this corresponds approximately to a damping ratio $\hat{\xi} = 0.5$. The constraint on the value of the cross-over frequency becomes

$$\omega_c \geq 0.154 \text{ rad/s} \tag{16.116}$$

If we select

$$\omega_c = 0.16 \text{ rad/s} \tag{16.117}$$

the corresponding natural frequency of the closed-loop system is

$$\omega_n = 0.126 \text{ rad/s} \tag{16.118}$$

and the proportional and derivative gains are given by

$$\begin{aligned} k_p &= \omega_n^2 = 0.0159 \\ k_d &= 2\xi\omega_n = 0.126 \end{aligned} \tag{16.119}$$

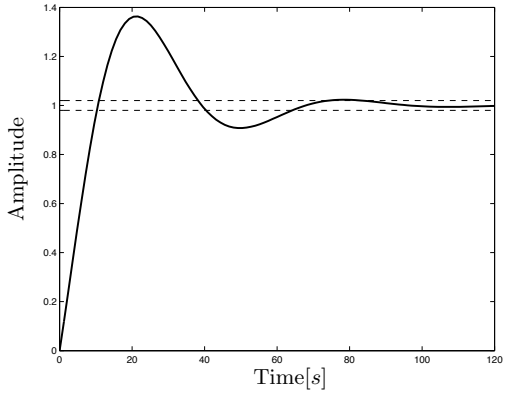

Figure 16.19 Closed-loop response to a unit step reference with a PD-control ($k_p = 0.0143$ and $k_d = 0.0957$).

It can be checked that this choice yields a satisfactory closed-loop response in terms of transient properties.

We have seen that the PD-control can be a good candidate for tracking a step reference with prescribed static and dynamic performances. However, its capability of rejecting measurement noise at high frequency is very poor. Indeed, the loop transfer function $L(j\omega)$ has a decay rate of only -20 dB/decade at high frequencies.

Moreover, if the system is subjected to a constant disturbance torque, the PD-control will reject it but with a steady-state error since the controller is lacking of an integral term. A remedy for this shortcoming is presented in the next section.

16.2.7 Proportional-derivative-integral (PID) control

The specification on zero steady-state error for a step disturbance can be satisfied by adding an integral term to the previous PD-control. The controller is typically called proportional-derivative-integral (PID) and the control law is expressed as

$$u(t) = k_p e(t) + k_d \dot{e}(t) + k_i \int_0^t e(\tau) d\tau \tag{16.120}$$

where k_i is the integral gain. The overall control action will be the result of the relative values of the three gains. The corresponding transfer function of the controller is given by

$$R(s) = k_p + s k_d + \frac{k_i}{s} \tag{16.121}$$

or, alternatively,

$$R(s) = \frac{s k_p + s^2 k_d + k_i}{s} \tag{16.122}$$

Accordingly, the open-loop transfer function is

$$L(s) = R(s)G(s) = \frac{k_i + s k_p + s^2 k_d}{s^3} \tag{16.123}$$

Let us verify first the static properties of the present control system. The steady-state error when a step disturbance is applied to the system is given by

$$e_{\text{ss}} = \lim_{s \to 0} s \frac{G(s)}{1 + L(s)} \frac{1}{s} = \lim_{s \to 0} s \frac{\frac{1}{s^2}}{1 + \frac{k_i + s k_p + s^2 k_d}{s^3}} \frac{1}{s} = \lim_{s \to 0} \frac{s}{s^3 + s^2 k_d + s k_p + k_i} = 0 \tag{16.124}$$

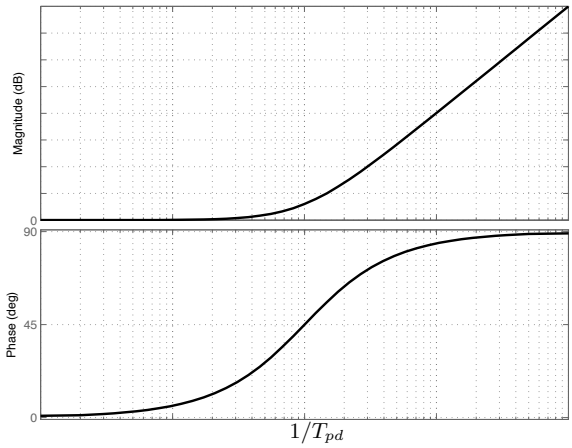

Figure 16.20 Bode diagram (magnitude and phase) of a PD-controller $R(s) = k(1 + sT_{pd})$ with $k = 1$.

irrespective of the values of the proportional, derivative and integral gain. Therefore, the PID-control is capable of rejecting a constant torque disturbance. The steady-state error when a step reference is applied to the system is given by

$$e_{\text{ss}} = \frac{1}{1 + \lim\limits_{s\to 0} L(s)} = \frac{1}{1 + \lim\limits_{s\to 0} \dfrac{k_i + sk_p + s^2 k_d}{s^3}} = \frac{1}{1+\infty} = 0 \tag{16.125}$$

irrespective of the values of the proportional, derivative and integral gain. Therefore, the PID-control is capable of tracking a step reference signal with zero steady-state error.

The design of the PID controller is then focused on the determination of the three gains such that the specifications on the transient response are met. We can proceed as follows. The controller may be written in an alternative form as

$$R(s) = k\,(1 + sT_{pd})\left(\frac{1 + sT_{pi}}{s}\right) \tag{16.126}$$

where

$$k_i = k \qquad k_d = kT_{pd}T_{pi} \qquad k_p = k\,(T_{pd} + T_{pi}) \tag{16.127}$$

Equation (16.126) shows that the controller transfer function is expressed as

$$R(s) = R_{pd}(s)R_{pi}(s) \tag{16.128}$$

where

$$R_{pd}(s) = k_{pd}\,(1 + sT_{pd}) \tag{16.129}$$

is the PD (porportional-derivative) part,

$$R_{pi}(s) = k_{pi}\left(\frac{1 + sT_{pi}}{s}\right) \tag{16.130}$$

is the PI (proportional-integral) part, and $k = k_{pd}k_{pi}$ is the product of the gain of the PD and PI part. The representation of the transfer function $R_{pd}(s)$ and $R_{pi}(s)$ is given, respectively, in Figure 16.20 and 16.21.

The following properties can be observed:

- The PD controller $R_{pd}(s)$ is characterized by a gain k_{pd} and a corner frequency at $\omega_c = 1/T_{pd}$.

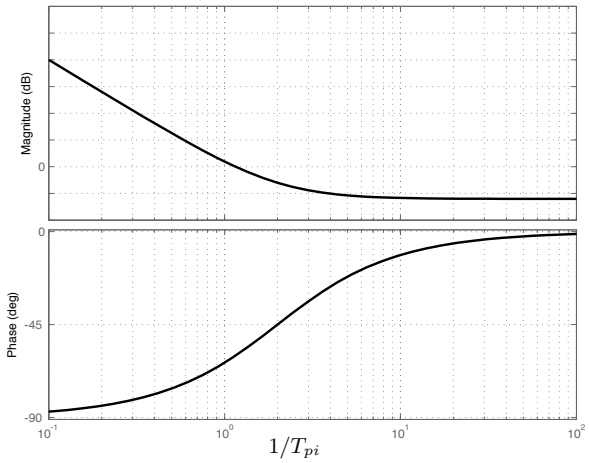

Figure 16.21 Bode diagram (magnitude and phase) of a PI-controller $R(s) = k\frac{1+sT_{pi}}{s}$ with $k = 1$.

- The PD controller adds positive phase (phase lead). This amount of phase can be computed as follows. Since $\angle R_{pd}(s) = \tan^{-1}(\omega T_{pd})$, the phase ϕ which is desired to be added with the PD controller at a specified frequency $\hat{\omega}$ is obtained by selecting

$$T_{pd} = \frac{\tan\phi}{\hat{\omega}} \tag{16.131}$$

- The PI controller $R_{pi}(s)$ is characterized by a gain k_{pi} and a corner frequency at $\omega_c = 1/T_{pi}$.
- The PI controller adds open-loop gain at low frequencies ($\omega \ll 1/T_{pi}$).
- The PI controller adds negative phase (phase lag). The amount of phase lag is close to -90^o when $\omega \ll 1/T_{pi}$ and it goes to zero for $\omega \gg 1/T_{pi}$.

Therefore, the PD part in Eq. (16.128) can be exploited to increase the phase margin, and consequently the damping ratio, due to the introduction of a phase lead. As seen above, an increase of phase margin is equivalent to a decrease in overshoot. On the other hand, the PI part can be used to improve the steady-state reference tracking and external disturbance rejection. If the corner frequency of $R_{pi}(s)$ is sufficiently small (i.e., T_{pi} is large), the phase lag introduced by the PI part is limited and does not affect too much cross-over and high frequency components of the open-loop frequency response.

The above considerations suggest to design our PID-control sequentially with a PD and a PI controller.

The PD-control part can be designed by referring to the previous section. We have seen that a satisfactory closed-loop response has been obtained by imposing a phase margin of 50^o, corresponding approximately to a cross-over frequency at 0.16 rad/s. With the aim of compensating the phase lag introduced by the PI part, let us impose a required phase for the PD part of the controller as

$$\phi = 60^o \text{ rad/s} \tag{16.132}$$

From Eq. (16.131), we find that

$$T_{pd} = \frac{\tan\phi}{\omega_c} = \frac{\tan 60^o}{0.16} = 10.83 \text{ s} \tag{16.133}$$

The PI-control part can be designed by selecting a corner frequency sufficiently small with respect to the assumed cross-over frequency. If a separation of one decade is chosen, we require that

$$T_{pi} = \frac{10}{\omega_c} = 62.5 \text{ s} \tag{16.134}$$

The overall gain of the controller in the form of Eq. (16.126) is selected such that $\omega_c = 0.16$ rad/s is actually the cross-over frequency of the system. Therefore, we must have

$$1 = |L(j\omega_c)| = k|G(j\omega_c)||1 + j\omega_c T_{pd}||\frac{1 + j\omega_c T_{pi}}{j\omega_c}| \tag{16.135}$$

which yields

$$k = 2.037 \times 10^{-4} \tag{16.136}$$

As a result, the controller gains are obtained as

$$k_p = 0.0150 \qquad k_d = 0.138 \qquad k_i = 2.037 \times 10^{-4} \tag{16.137}$$

It can be seen that the closed-loop step response to a unit reference with the gain values computed above is characterized by a maximum percentage overshoot of 31%, which slightly exceeds our specification. Similarly to what done for the PD-control, we could reduce the overshoot by increasing the derivative action. Let's try with the following choice

$$k_p = 0.0150 \qquad k_d = 0.150 \qquad k_i = 2.037 \times 10^{-4} \tag{16.138}$$

The corresponding PID controller and loop transfer function are given by

$$R(s) = 0.0150 + 0.150s + \frac{0.0002037}{s} \tag{16.139}$$

and

$$L(s) = \frac{0.0002037 + 0.015s + 0.15s^2}{s^3} \tag{16.140}$$

The loop function has three poles at the origin, i.e.,

$$p_{1,2,3} = 0 \tag{16.141}$$

and two real zeros at

$$z_1 = -0.0162 \qquad z_2 = -0.0838 \tag{16.142}$$

The Bode plot of $L(s)$ is represented in Figure 16.22, with a cross-over frequency of approximately 0.168 rad/s and a phase margin of approximately 58 degrees.

The step response is shown in Figure 16.23, where it can be observed that all the transient specifications are met.

As a final remark, the attitude response to a step torque disturbance with the previously designed PID-control is shown in Figure 16.24.

16.2.8 PID control with improved high-frequency noise rejection

The PID-control presented so far is capable of satisfying the first five requirements listed in Section 16.2.4. However, as clearly shown in Fig. 16.22, the high-frequency decay rate is only -20 dB/decade. This is in contrast with the last specification, which requires to have a decay rate of -40 dB/decade in order to achieve a good measurement noise rejection. A PID control with improved high-frequency noise rejection can be obtained by adding a real pole to the controller transfer function. This leads to

$$R(s) = \frac{s^2 k_d + s k_p + k_i}{s\,(1 + sT_n)} \tag{16.143}$$

where T_n should be selected to increase the decay rate above a prescribed frequency without affecting too much the magnitude and phase in the cross-over region. In this way, we could use the PID gains designed above to maintain the transient performances. This can be achieved if the additional pole is well separated from the cross-over frequency region. Let us try with a pole at 3 rad/s (more than one decade above the cross-over frequency 0.168 rad/s). This corresponds to $T_n = 0.333$. The resulting controller has the form

$$R(s) = \frac{0.0002037 + 0.015s + 0.15s^2}{s\,(1 + 0.333s)} \tag{16.144}$$

The Bode diagram of the loop transfer function is shown in Figure 16.25, where the phase margin is approximately 55 degrees and the cross-over frequency is practically unaffected with respect to the simple PID control. It can be seen that the closed-loop step response to a unit reference satisfies again all the transient specifications.

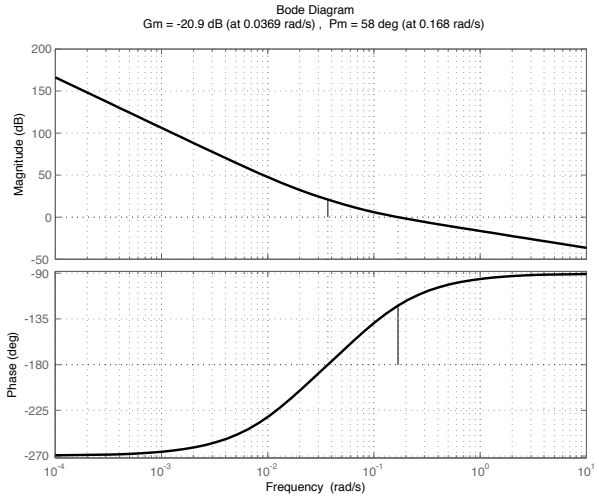

Figure 16.22 Bode diagram (magnitude and phase) of $L(s)$ with a PID-control.

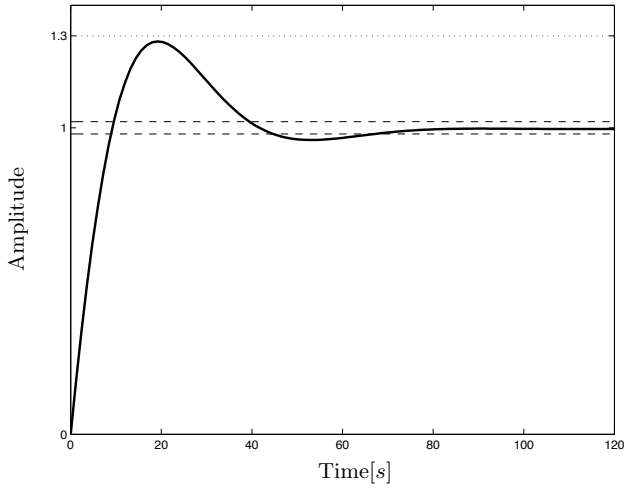

Figure 16.23 Closed-loop response to a unit step reference with a PID-control.

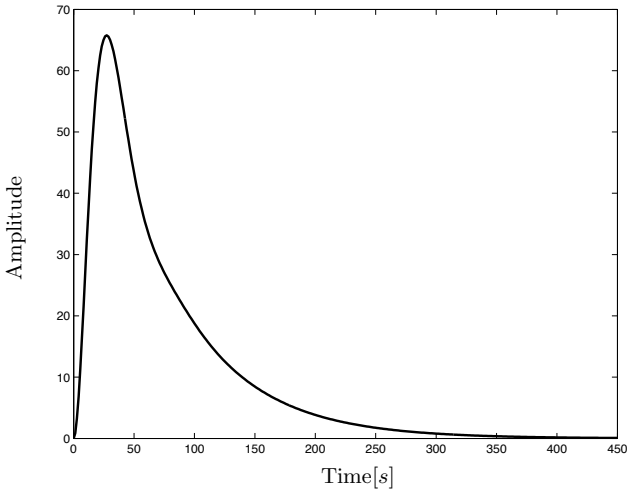

Figure 16.24 Closed-loop response to a unit step disturbance with a PID-control.

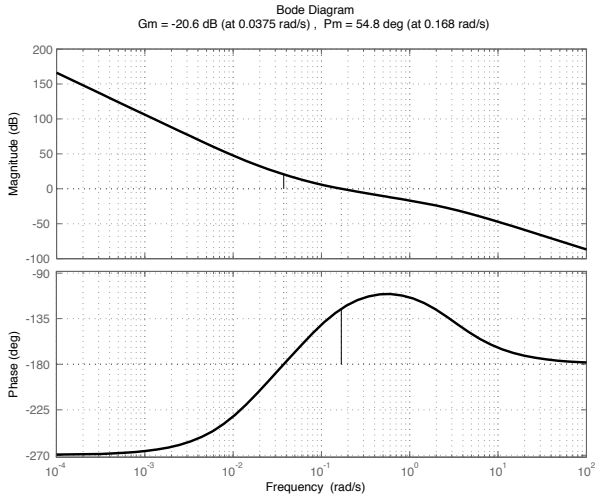

Figure 16.25 Bode diagram (magnitude and phase) of $L(s)$ with a PID-control including an additional high-frequency pole to improve the noise rejection.

16.2.9 Effects of actuator dynamics

The model used until now to design the attitude control system is based on the assumption that the torque actuator is ideal, i.e., it is capable to provide the torque imposed by the controller whatever is the amplitude and the operating frequency. In other words, the actuator has been assumed to be of infinite power and infinite bandwidth. In practice, this is not true since, as any real device, it has some power limitations which prevent to achieve arbitrarily large torques and it is characterized by an internal dynamics which limits its bandwidth.

As previously mentioned, one way of enforcing that the control law will not demand more torque than the actuator is capable of is to provide an additional restriction on the closed-loop poles locations, i.e., the poles can be moved from open-loop to closed-loop locations to achieve some desired performances but the distance between closed-loop and open-loop locations must not exceed a prescribed quantity which is related to the actuator power.

A band-limited actuator can be represented by an additional dynamic model, which is typically expressed by a transfer function having as output variable the actual torque and as input variable the torque commanded by the control law, i.e.,

$$u(s) = A(s)u_c(s) \tag{16.145}$$

where $A(s)$ contains the dynamics of the actuator. In order to perform a numerical analysis, one must select an appropriate $A(s)$ which reasonably represents the behavior of the control device. For example, if we assume that our satellite is equipped with a reaction wheel, a reasonable actuator model is the first-order transfer function

$$A(s) = \frac{1}{1 + sT_a} \tag{16.146}$$

where $T_a > 0$ is the time-constant of the actuator.

16.2.10 Effects of flexibility

Let consider the case where the appendages are flexible. The linearized dynamics of the system will be expressed by a new transfer function $G(s)$ which is derived as follows.

First, the transverse displacement of each tip mass is expressed as

$$s(t) = \ell\theta(t) + w(t) \tag{16.147}$$

where $w(t)$ is the small displacement relative to the rigid-body rotational motion induced by the flexibility of the beam (see Fig 16.1). Accordingly, the kinetic energy of the flexible spacecraft is given by

$$\begin{aligned} T &= \frac{1}{2}J_0\dot{\theta}^2 + 2\frac{1}{2}m\left(\ell\dot{\theta} + \dot{w}\right)^2 \\ &= \frac{1}{2}\left(J_0 + 2m\ell^2\right)\dot{\theta}^2 + 2\frac{1}{2}m\dot{w}^2 + 2m\ell\dot{\theta}\dot{w} \end{aligned} \tag{16.148}$$

Since the appendages are flexible, we also have a potential energy given by

$$V = 2\frac{1}{2}k_a w^2 \tag{16.149}$$

where

$$k_a = \frac{3EJ}{\ell^3} \tag{16.150}$$

is the equivalent stiffness of a massless cantilever beam of bending rigidity EJ carrying a tip point mass. Considering some small damping of the flexible appendage, we can write a dissipation function as

$$D = 2\frac{1}{2}c_a\dot{w}^2 \tag{16.151}$$

where c_a is the viscous damping coefficient representing the energy dissipation due to the vibration of each appendage.

Using Lagrange's equations, the linearized equations of motion of the system are the following

$$\begin{aligned} &J\ddot{\theta} + 2m\ell\ddot{w} = T_c \\ &2m\ddot{w} + 2m\ell\ddot{\theta} + 2c_a\dot{w} + 2k_a w = 0 \end{aligned} \tag{16.152}$$

In the Laplace domain, we can write

$$\begin{aligned} s^2 J\theta(s) + 2m\ell s^2 w(s) &= T_c(s) \\ \left(s^2 m + sc_a + k_a\right) w(s) + m\ell s^2\theta(s) &= 0 \end{aligned} \tag{16.153}$$

From the second equation

$$w(s) = -\frac{s^2 m\ell}{s^2 m + sc_a + k_a}\theta(s) \tag{16.154}$$

Therefore, the first equation becomes

$$\left[s^2 J - \frac{s^4 2m^2\ell^2}{s^2 m + sc_a + k_a}\right]\theta(s) = T_c(s) \tag{16.155}$$

or, alternatively,

$$\frac{s^2 J\left(s^2 m + sc_a + k_a\right) - s^4 2m^2\ell^2}{s^2 m + sc_a + k_a}\theta(s) = T_c(s) \tag{16.156}$$

Accordingly, the attitude angle is related to the input control torque by

$$\begin{aligned} \theta(s) &= \frac{s^2 m + sc_a + k_a}{s^2 J\left(s^2 m + sc_a + k_a\right) - s^4 2m^2\ell^2} T_c(s) \\ &= \frac{1}{s^2 J}\frac{s^2 m + sc_a + k_a}{s^2\left(m - \frac{2m^2\ell^2}{J}\right) + sc_a + k_a} T_c(s) \\ &= \frac{1}{s^2 J}\frac{s^2 m + sc_a + k_a}{s^2 m\frac{J_0}{J} + sc_a + k_a} T_c(s) \\ &= \frac{1}{s^2 J}\frac{s^2 + 2\xi_a\omega_a s + \omega_a^2}{s^2\frac{J_0}{J} + 2\xi_a\omega_a s + \omega_a^2} T_c(s) \end{aligned} \tag{16.157}$$

In more compact notation,

$$\theta(s) = \frac{1}{s^2 J_0}\frac{s^2 + 2\xi_a\omega_a s + \omega_a^2}{s^2 + (1+\mu)2\xi_a\omega_a s + (1+\mu)\omega_a^2} T_c(s) \tag{16.158}$$

where

$$\mu = \frac{2m\ell^2}{J_0} \tag{16.159}$$

Using the classical control notation we can write

$$y(s) = G_{\text{flex}}(s)u(s) \tag{16.160}$$

where

$$G_{\text{flex}}(s) = \frac{1}{s^2 J_0}\frac{s^2 + 2\xi_a\omega_a s + \omega_a^2}{s^2 + (1+\mu)2\xi_a\omega_a s + (1+\mu)\omega_a^2} \tag{16.161}$$

is the system transfer function when the appendages are modelled as massless flexible beams carrying a tip point mass.